Acoustic surveys of euphausiids and models of baleen whale distribution in the Barents Sea

P. H. Ressler[1,2,*], P. Dalpadado[2], G. J. Macaulay[2], N. Handegard[2], M. Skern-Mauritzen[2]

[1]**Alaska Fisheries Science Center, NOAA National Marine Fisheries Service, Seattle, WA 98115, USA**
[2]**Institute of Marine Research (IMR), PO Box 1870 Nordnes, 5817 Bergen, Norway**

ABSTRACT: As in many high-latitude ecosystems, euphausiids (order Euphausiacea, 'krill') play a key role in the Barents Sea by channeling energy from primary producers to fish and other zooplankton predators. We used multifrequency acoustic data from several recent multidisciplinary surveys to describe the spatial distribution of backscatter likely to be from euphausiids. Spatial patterns in euphausiid backscatter observed in 2010, 2011, and 2012 were correlated with vertically integrated euphausiid biomass collected with plankton nets, and were also broadly consistent with the distribution of euphausiids expected from the literature. We used the high-resolution and broad-spatial coverage of our euphausiid backscatter data to update multiple regression models of baleen (fin, humpback, and minke) whale distribution to test the hypothesis that these animals aggregated where euphausiids were abundant. After controlling for physical environmental factors and the densities of capelin and several other potential prey taxa, we found that fin whale densities were positively and linearly associated with euphausiid backscatter, and higher than average densities of humpback whales were found in areas with high euphausiid backscatter. No association was found between minke whales and euphausiids. Densities of all 3 whale species were also positively associated with capelin. For fin and humpback whales, the effects of capelin and euphausiids on whale densities appeared to be principally separate and additive, although there was some evidence for a stronger effect of euphausiids at low capelin densities. In terms of their preference for euphausiids and capelin, these whale species appeared to be flexible, opportunistic predators.

KEY WORDS: Euphausiids · Capelin · *Thysanoessa* · Minke whale · Fin whale · Humpback whale · Acoustics · Barents Sea

INTRODUCTION

The Barents Sea ecosystem includes the continental shelf bordering northern Norway and Russia, with latitudes ranging from ca. 68 to 82° N, an area of 1.6 million km², and an average depth of 230 m (Fig. 1). Warm Atlantic water enters predominantly from the southwest, while cold Arctic water dominates in the northeast. The Barents Sea is inhabited by a mixture of Arctic and Atlantic species, including some of the world's largest stocks of cod *Gadus morhua*, capelin *Mallotus villosus*, and haddock *Melanogrammus aeglefinus*, and is the main nursery ground for the large stock of Norwegian spring-spawning herring *Clupea harengus* (Olsen et al. 2010). Euphausiids ('krill') play a key role in the Barents Sea by channeling energy from primary producers (phytoplankton) to cod, capelin, haddock, herring, polar cod *Boreogadus saida*, and other predators of zooplankton (Skjoldal et al. 2004, Dolgov et al. 2011). In particular, capelin is a key planktivore, euphausiid consumer, and forage fish, with a trophic
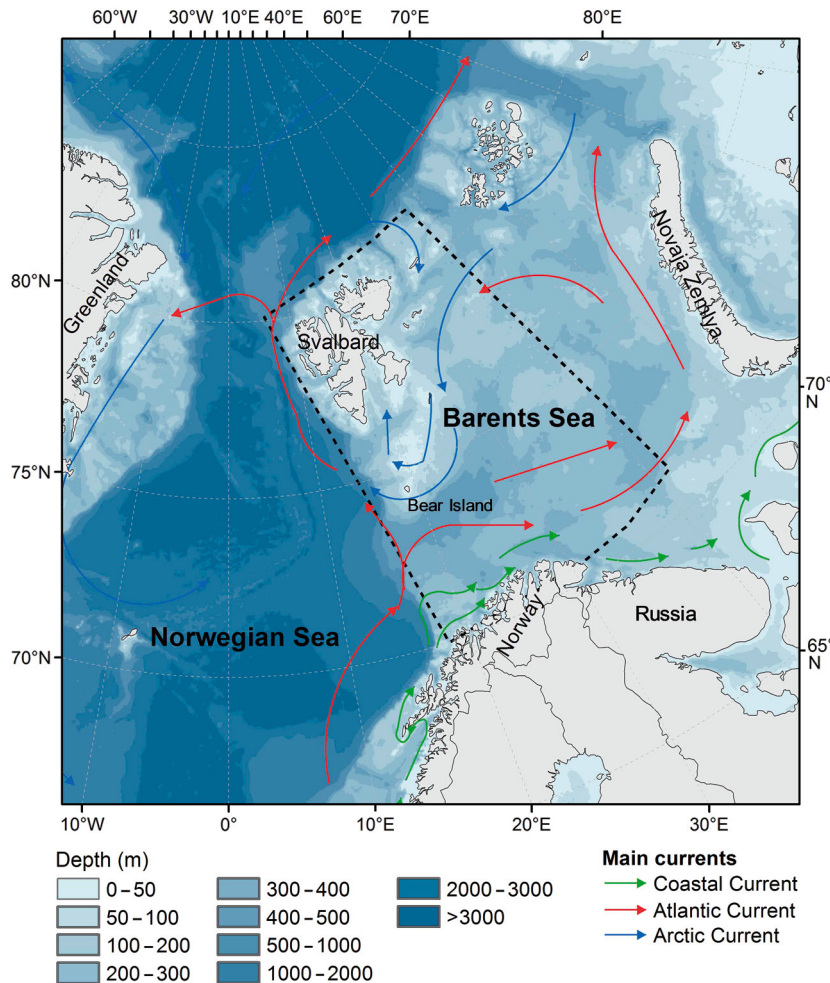
Fig. 1. Barents Sea ecosystem survey area. Color shading indicates bottom depth, and prevailing current flows are indicated by colored arrows. The black dashed-line polygon indicates the approximate area covered by Norwegian vessels as part of the Barents Sea ecosystem survey, 2010–2012

ents Sea and is thus available as a principal food source to higher trophic levels (Dalpadado & Skjoldal 1991, 1996, Drobysheva 1994). The neritic, cold water-associated *Thysanoessa raschii* dominates the south-eastern part of the Barents Sea (Drobysheva 1994) and is less important as a food source. *Meganyctiphanes norvegica*, the largest species in terms of body size, has historically been of minor importance in terms of abundance and as prey in the Barents Sea (though it is abundant in the neighboring Norwegian Sea ecosystem); it has become more common in the Barents Sea during the warmer conditions of recent years (Zhukova et al. 2009, Norwegian Institute of Marine Research [IMR] unpubl. data). The distribution of euphausiids is generally characterized by patchy areas of higher concentrations in the central Barents Sea and around Svalbard (Zhukova et al. 2009, Eriksen & Dalpadado 2011, Skern-Mauritzen et al. 2011). Annual changes in the abundance and distribution of euphausiids are thought to be driven by the amount of inflow of Atlantic water from the Norwegian Sea and by predation pressure from capelin and other predators (Dalpadado & Skjoldal 1996, Zhukova et al. 2009, Dalpadado et al. 2012).

Two main time series of euphausiid data from plankton net collections exist in the Barents Sea. Euphausiids have been collected since 2003 as part of a suite of biological and physical observations made during multidisciplinary Norwegian-Russian ecosystem surveys in the Barents Sea that occur from August to early October (Olsen et al. 2011, Michalsen et al. 2013), taken either as incidental catch in surface trawls for age-0 pelagic fishes (Eriksen & Dalpadado 2011) or occasionally with depth-stratified MOCNESS samples (Dalpadado & Skjoldal 1991, 1996, Dalpadado et al. 2012). In addition, there is a long time series (1952 to the present) of euphausiid catches in late autumn to winter using very small (0.2 m², 0.564 mm mesh) plankton nets attached to bottom trawls (Zhukova et al. 2009, Orlova et al. 2011). Sampling euphausiids with nets provides physical samples with high taxonomic resolution. However, euphausiids may avoid or be extruded from the meshes of various types of

role that is further magnified by great variability in its stock size (Johannesen et al. 2012). Capelin and euphausiids have overlapping spatial distributions, and when the capelin stock is large, capelin exert high predation pressure on euphausiids, in particular, as well as on other zooplankton (Dalpadado & Skjoldal 1996, Orlova et al. 2002, Dalpadado & Mowbray 2013). Both capelin and euphausiids are important in the diets of Barents Sea minke whales *Balaenoptera acutorostrata* (Skaug et al. 1997, Haug et al. 2002, Smout & Lindstrøm 2007) and perhaps of fin whales *B. physalus* and humpback whales *Megaptera novaeangliae* as well (Jonsgård 1966, Christensen et al. 1992, Skern-Mauritzen et al. 2011).

The Barents Sea euphausiid community is represented by 6 species (Orlova et al. 2011). The most abundant, *Thysanoessa inermis*, is predominantly a herbivore; it dominates the central and northern Bar-

towed samplers (Clutter & Anraku 1968, Sameoto et al. 1993, 2000, Wiebe et al. 2013), and the spatial resolution of sampling with these gear types is limited. The sampling gear used in the Barents Sea time series reported in Eriksen & Dalpadado (2011) and Zhukova et al. (2009) is probably not optimal for capturing euphausiids, and, due to these methodological problems, knowledge of standing stock and distribution is limited (Eriksen & Dalpadado 2011).

In contrast to plankton nets, acoustic techniques offer a higher sampling rate at a relatively coarser taxonomic resolution by separating groups of animals of different sizes and frequency-dependent acoustic properties; they are often used in tandem with net or optical sampling to confirm size and species composition of detected targets (Holliday & Pieper 1995, Horne 2000, Simmonds & MacLennan 2005). If euphausiids can reliably be distinguished from other zooplankton and from fish (especially fish larvae/juveniles) on the basis of relative backscatter response among multiple acoustic frequencies, these techniques can provide high-resolution distribution and abundance (or biomass) survey data for this important group of zooplankton at a large spatial scale (Korneliussen & Ona 2003, De Robertis et al. 2010). Acoustic surveys have been used to create quantitative survey time series of euphausiid biomass in the Antarctic (*Euphausia superba*; Brierley et al. 1997, Hewitt & Demer 2000, Hewitt et al. 2004, Reiss et al. 2008), and, more recently, in the Bering Sea (*Thysanoessa* spp.; Ressler et al. 2012). Acoustic studies in field (e.g. Kristensen & Dalen 1986, Klevjer & Kaartvedt 2006, Calise 2009, Ferreira et al. 2012) and experimental settings (Calise & Knutsen 2012) have been conducted on the euphausiids *M. norvegica* from Norwegian waters, but acoustic surveys of Barents Sea euphausiids have not been conducted.

One potential application of data from high-resolution, large-scale acoustic surveys of euphausiid abundance or biomass in the Barents Sea is in models of the mesoscale interaction and predator–prey dynamics of euphausiids and their predators. During late summer feeding migrations in the northern Barents Sea, baleen whales are thought to mainly feed on capelin and euphausiids, though it is not clear whether they exert a preference for one prey type over the other (Lindstrøm et al. 1997, Skaug et al. 1997, Harbitz & Lindstrøm 2001, Lindstrøm & Haug 2001, Haug et al. 2002). Skern-Mauritzen et al. (2011) created statistical models of minke, fin, and humpback whales in this system and hypothesized that these animals were diet generalists rather than specialists, feeding on both pelagic fish (e.g. capelin)

and zooplankton prey (e.g. euphausiids) and therefore aggregating where both of these prey species were abundant. However, because data on euphausiid abundance or biomass were not available at the same resolution as data on pelagic fishes obtained from acoustic-trawl surveys at the time of their study, they were unable to test the relative importance of euphausiids as a predictor of whale distribution.

Although the Barents Sea ecosystem surveys were not specifically designed to map euphausiid distribution, the acoustic backscatter data from these surveys are suitable for that purpose. Here, we use acoustic backscatter data collected during 3 recent Barents Sea ecosystem surveys (2010, 2011, and 2012) to create a high-resolution index of the distribution and biomass of euphausiids. We show euphausiid backscatter distributions for the 3 yr, and compare our results to euphausiid biomass and distribution from net catches. Finally, we add these euphausiid data as an additional covariate to the whale distribution models of Skern-Mauritzen et al. (2011) to (1) test the hypothesis that these animals aggregate where euphausiids are abundant, which would be consistent with the previously proposed predator–prey relationship, and (2) evaluate the relative importance of both euphausiids and capelin as drivers of whale distributions.

MATERIALS AND METHODS

Description of data sets

The data analyzed here were collected during 3 recent Barents Sea ecosystem surveys using combinations of 4 Norwegian survey vessels, as follows: (1) 'Johan Hjort', 'G.O. Sars', and 'Helmer Hanssen', 23 August to 23 September 2010; (2) 'Johan Hjort', 'Christina E.', and 'Helmer Hanssen', 9 August to 30 September 2011; and (3) 'Johan Hjort', 'G.O. Sars', and 'Helmer Hanssen', 16 August to 28 September 2012. Data from all vessels were combined for the analysis in each year, assuming that together they constituted one synoptic survey of the study area. More details concerning these surveys are available from Olsen et al. (2011) and Michalsen et al. (2013). Here, we focus principally on acoustic data and net sampling of euphausiids collected in the Norwegian sector of the Barents Sea (Fig. 1). Simrad EK60[1] scientific echosounders (Kongsberg Maritime AS) with

---

[1]Reference to trade names does not imply endorsement

transducers located on retractable centerboards at 6 to 8 m depth were used to continuously collect acoustic backscatter data along predetermined survey transects. The frequencies used included 18, 38, 70, 120, 200, and 333 kHz, allowing the backscatter frequency response of euphausiids to be observed; the available frequencies varied by vessel and survey. Echosounders were calibrated using a standard sphere (Foote et al. 1987). Average sound speed and acoustic absorption values from conductivity-temperature-depth (CTD) casts were used for acoustic data processing. Sampling rate varied with bottom depth, but was nominally 4 pings s^{-1}, and vessel speed along survey transects was typically 8 to 12 knots (4 to 6 m s^{-1}). The bottom depth on most transects was between 50 and 400 m. Net samples of plankton including euphausiids were collected with a MOC-NESS (multiple opening-closing net environmental sensing system; Wiebe et al. 1975) with 1 m^2 mouth area, 0.180 mm mesh, up to 8 nets, towed at 1.5 to 2 knots (0.8 to 1 m s^{-1}) and a single-net macroplankton trawl with 36 m^2 mouth area and 3 mm mesh towed at 2 to 3 knots (1 to 1.5 m s^{-1}) (Heino et al. 2011, W. Melle et al. unpubl.) that was not used in previous ecosystem surveys. We did not use incidental euphausiid catch from surface trawls for age-0 pelagic fishes (Eriksen & Dalpadado 2011), nor from very small plankton nets not designed to capture large zooplankton such as euphausiids quantitatively.

Acoustic data processing and classification

Data were processed using Echoview (Myriax) and Matlab (The Mathworks) software packages. Range-dependent background noise and signal-to-noise ratio (SNR) were estimated for 120 kHz and higher frequencies using the method of De Robertis & Higginbottom (2007). For 18 kHz, noise from transducer ringing and possibly reverberation within the retractable centerboard (E. Ona, IMR, pers. comm.) present at shorter ranges (20 to 50 m) was regressed on depth, and the resulting fit was used to compute SNR of the observed volume backscatter data (S_v), as in De Robertis et al. (2010). It was assumed that 38 and 70 kHz S_v had a >10 dB SNR at the ranges analyzed here (De Robertis & Higginbottom 2007). A bottom offset of 2 m from the depth of the average sounder-detected bottom echo at all available frequencies was used to ensure the exclusion of any backscatter from the seafloor (a small amount of euphausiid backscatter very close to the seafloor may have sometimes been excluded as well); data were sub-

sequently screened for unusually large values that could indicate integration of the bottom echo. Since the vessel-mounted echosounders likely underestimate euphausiid backscatter during nighttime due to vertical migration toward the surface, above the transducers (Ressler et al. 2012), backscatter data collected at night were excluded from this analysis. Only data collected while a vessel was moving along survey transects (and not those collected during station operations) were used.

Euphausiids of the sizes and species present in this system are relatively weak acoustic targets (ca. −70 to −90 dB at 120 kHz; e.g. Greenlaw 1979, Kristensen & Dalen 1986, Klevjer & Kaartvedt 2006, Calise & Knutsen 2012, Smith et al. 2013), so SNR ratio requirements for acoustic classification are demanding. Particularly at frequencies above 120 kHz, signal attenuation increases substantially with range and lowers SNR (Korneliussen 2000, De Robertis & Higginbottom 2007); at the lowest frequency, 18 kHz transducer ringing at short ranges and multiple bottom echoes also lowered SNR. In this data set, 38 and 120 kHz were the only acoustic frequencies that (1) were common to all vessels and survey years and (2) had a SNR consistently >10 dB over the ranges analyzed here. Thus, only the difference between S_v at 120 and 38 kHz ($\Delta S_{v,120-38} = S_{v,120} - S_{v,38}$) was used for classification of euphausiid backscatter.

Euphausiid backscatter was classified (Fig. 2) using the method described in detail by De Robertis et al. (2010) and Ressler et al. (2012). Briefly, acoustic volume backscatter data (S_v, dB re 1 m^{-1}) were averaged into 5 ping by 5 m cells, and then the Z-score defined as

$$Z_{120-38,\text{euph},l} = \left| \frac{\Delta S_{v120-38,l} - \mu_{120-38,\text{euph}}}{\sigma_{120-38,\text{euph}}} \right| \qquad (1)$$

was computed for each cell l, where $\mu_{120-38,\text{euph}}$ and $\sigma_{120-38,\text{euph}}$ are the mean and standard deviation of $\Delta S_{v,120-38}$, respectively, collected at locations and depths where pure catches of euphausiids had been obtained.

Cells containing backscatter with a SNR > 10 dB were classified as follows:

$$S_{v,\text{euph},l} = \begin{cases} S_{v,\text{euph}} & \text{if} \quad Z_{120-38,\text{euph},l} \leq Z_{\text{thresh}} \\ -999 & \text{if} \quad Z > Z_{\text{thresh}} \end{cases} \qquad (2)$$

where Z_{thresh} is the threshold value used to provisionally classify the cell as euphausiids. We have used $Z_{\text{thresh}} = 2$, which will include observations within approximately 2 standard deviations of $\mu_{120-38,\text{euph}}$.

Provisional classifications as $Z_{120-38,\text{euph}}$ were subsequently smoothed by computing the mean at a

$$Z_{120-38,\text{euph},l} = \left| \frac{\Delta S_{v,120-38,l} - \mu_{120-38,\text{euph}}}{\sigma_{120-38,\text{euph}}} \right|$$
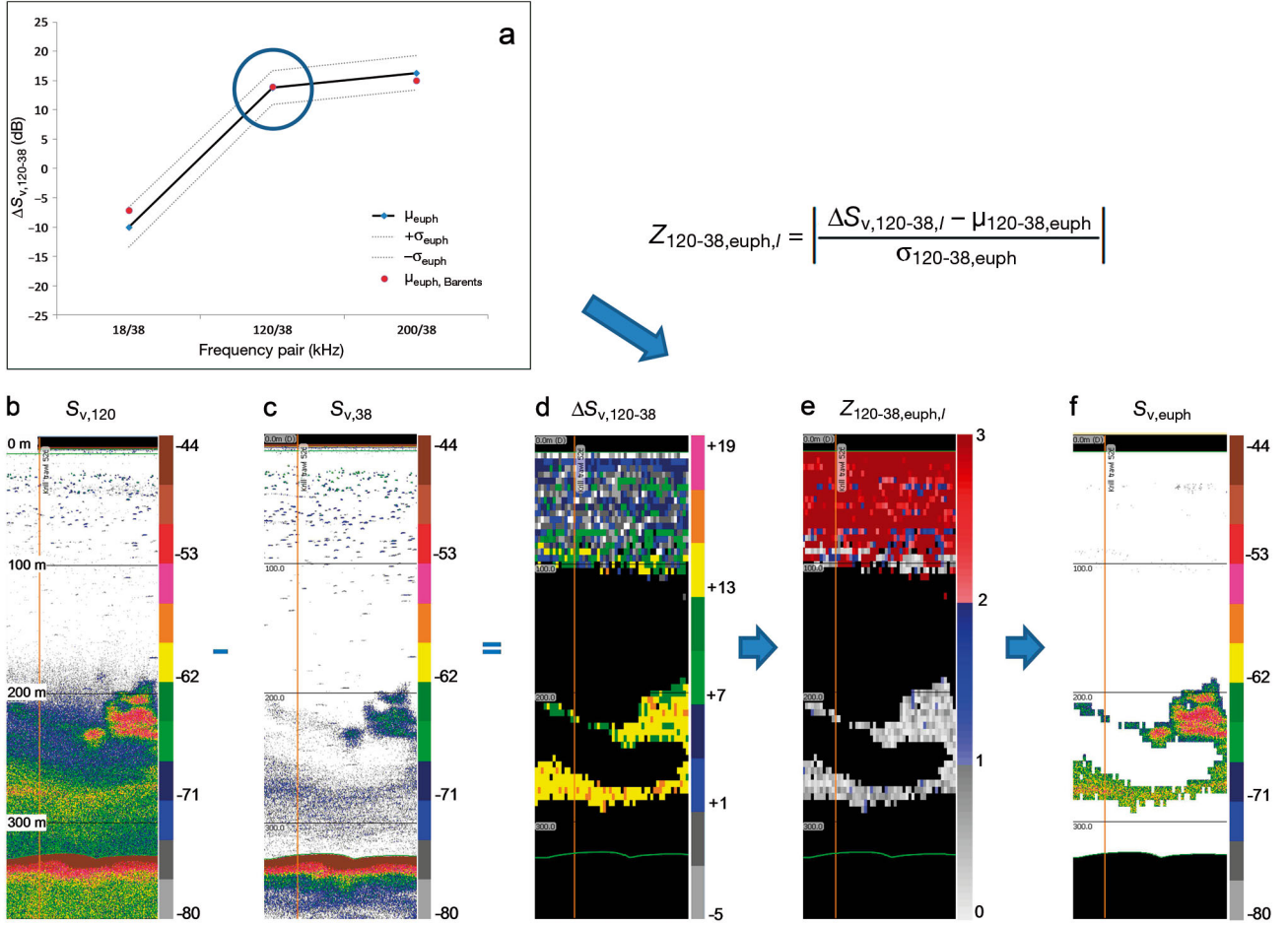
Fig. 2. Illustration of the methodology. (a) The frequency response from the trawl path of the targeted macroplankton trawl conducted during the 2011 survey with RV 'Johan Hjort' is shown as red circles. Blue diamonds and solid black line indicate the frequency response from 27 tows whose catches were comprised almost entirely of *Thysanoessa* spp. euphausiids (De Robertis et al. 2010); the dotted lines indicate $\pm 1\sigma_{\text{euph}}$. $\mu_{120-38,\text{euph}}$ and $\sigma_{120-38,\text{euph}}$ are used when calculating $Z_{120-38,\text{euph}}$. (b,c) Echograms (acoustic backscatter by depth along a survey transect) showing $S_{v,120}$ and $S_{v,38}$ respectively; white color indicates S_v below the color scale minimum. (d) The difference between S_v at 2 frequencies, $\Delta S_{v,120-38}$. Backscatter very close to the transducer and below the seafloor (indicated by a green line) has been excluded in this echogram; black color within the water column indicates where the signal-to-noise ratio (SNR) of $S_{v,120}$ is <10. Note that some euphausiid-like backscatter between 200 m and the seafloor is excluded due to low SNR. (e) $Z_{120-38,\text{euph}}$, the Z-score used for classifying the euphausiid backscatter. (f) $S_{v,120}$ echogram masked using a $Z_{120-38,\text{euph}}$ threshold of 1.5 to produce an echogram showing euphausiid backscatter, $S_{v,\text{euph}}$

coarser cell resolution, 0.5 nautical miles (nmi; 926 m) by 20 m, and then applying Eq. (2) using a Z_{thresh} of 1.5. This effectively allowed backscatter to be classified as euphausiids only when the frequency responses of other nearby cells were also consistent with euphausiids (cf. De Robertis et al. 2010). Finally, $S_{v,\text{euph}}$ at 120 kHz in these larger 0.5 nmi by 20 m cells was integrated using an S_v threshold of −80 dB, and $S_{v,\text{euph}}$ was vertically integrated over the water column and expressed as $s_{A,\text{euph}}$ (m² nmi⁻²) for each 0.5 nmi EDSU (elementary distance sampling unit). A weighted water-column average of $Z_{120-38,\text{euph}}$ was computed for each EDSU, using the euphausiid backscatter in each 0.5 nmi by 20 m cell as the weights; these values were examined to evaluate the consistency of backscatter classification within and among surveys.

Frequency response of euphausiids

Targeted net sampling of suspected euphausiid scattering layers for purposes of verification and empirical determination of acoustic frequency response was not a regular part of 2010–2012 ecosystem surveys, and only one such tow was conducted with the new macroplankton trawl by RV 'Johan Hjort' in 2011. The frequency response of euphausiids sam-

pled by this trawl was analyzed by computing the mean $\Delta S_{v,18-38}$, $\Delta S_{v,120-38}$, and $\Delta S_{v,200-38}$, from the path of the trawl, using the 5 m by 5 ping block averages with >10 dB SNR as the unit of sampling. A more extensive data set collected on euphausiids of the same genus from the Bering Sea and analyzed in the same manner (De Robertis et al. 2010) was (1) evaluated for consistency with backscatter from the trawl path of this single 2011 targeted macroplankton trawl and (2) used to provide $\mu_{120-38,euph}$ and $\sigma_{120-38,euph}$ for the acoustic classification procedure (Fig. 2).

Comparison with euphausiid biomass from MOCNESS sampling

MOCNESS tows were made at a limited number of predetermined stations during the 2010, 2011, and 2012 surveys. MOCNESS catches were divided into 2 halves: one half was preserved in seawater-buffered 4% formalin for analysis of species composition and abundance at the IMR laboratory, and the other half was used for biomass estimation. The half sampled for biomass was fractionated successively through 3 sieves: 2 mm, 1 mm, and 180 μm. The content on each sieve was briefly rinsed with freshwater (to remove salt) and transferred to pre-weighed aluminium trays. The biomass, species, and size composition of euphausiids reported here is for animals sorted from the >2 mm fraction and analyzed on board. The weight of euphausiids was obtained after drying these animals at 60°C for a minimum of 24 h (until the weight was constant). Results were expressed as dry weight biomass per square meter of water column (g m^{-2}) by taking into account the volume of water filtered through each depth-stratified net sample and vertically integrating over all nets.

MOCNESS nets were never targeted on acoustic scattering layers from euphausiids or any other taxa, and thus were not appropriate for empirically determining the frequency response of single taxa as in De Robertis et al. (2010). However, we were able to compare the spatial pattern of vertically integrated euphausiid biomass from MOCNESS samples to the spatial distribution of $s_{A,euph}$, hypothesizing that $s_{A,euph}$ at a given location would be a good index of euphausiid biomass there. Daytime $s_{A,euph}$ values were averaged within 5 nmi of each nighttime MOC-NESS station in each Barents Sea ecosystem survey data set for which the acoustic analysis was available (2010, 2011, and 2012); for example, daytime $s_{A,euph}$ used for the average might correspond to the location

of a MOCNESS tow conducted during station work on the previous night. $s_{A,euph}$ from daytime was compared with MOCNESS catch biomass (g m^{-2}) from nighttime tows because these are the diel periods when each method is most effective: net avoidance by euphausiids is likely to be most severe during daytime (Clutter & Anraku 1968, Smith 1991, Sameoto et al. 1993, 2000, Coyle & Pinchuk 2002, Wiebe et al. 2013), and, as noted previously, acoustic methods may underestimate euphausiid backscatter at night (Ressler et al. 2012). A functional regression (which allows for error in both series; Ricker 1973) was fit to the data to assess the null hypothesis of no relationship between the 2 series.

Modeling the spatial distribution of whales

The euphausiid backscatter observations obtained with the method outlined above were used as an additional predictor in an existing model framework for the spatial distribution of whales in the Barents Sea (cf. Skern-Mauritzen et al. 2011). Routine ecosystem survey data collection methods for determining the abundance and distribution of baleen whales and their pelagic fish prey are described in more detail elsewhere (Olsen et al. 2011, Skern-Mauritzen et al. 2011) and are only briefly summarized here. The number and position of all marine mammals including baleen whales within ±45° of the vessel track were recorded by 2 visual observers on the bridge of each vessel, as sighting conditions permitted during Barents Sea ecosystem surveys (visibility and sea state were recorded continuously). Also, the distribution of acoustic backscatter from pelagic fishes such as capelin, herring, polar cod, and blue whiting *Micromesistius poutassou* was determined by trained analysts using standard survey procedures, including visual scrutiny of acoustic backscatter data and the species and size composition from targeted pelagic trawl catches. Following Skern-Mauritzen et al. (2011), whale sightings (in number km^{-1}; total no. of sightings in our study—minke whales: n = 271; humpback whales: n = 619; fin whales: n = 234) and acoustic backscatter densities of prey species (euphausiids [contributed by this study], capelin, herring, polar cod, and blue whiting; s_A, m^2 nmi^{-2}) from 2010 to 2012 were summarized into grid cells of 50 × 50 km for statistical modeling. To better visualize the general spatial distribution of the whales and each potential prey covariate, generalized additive mixed models (GAMMs) were separately fit for each species in the form of:

$$D_{ij} \sim \text{factor(year}_j) + s(\text{depth}_{ij}) + s(X_{ij}, Y_{ij}) + e_{ij} \quad (3)$$

and predictions from these models were then displayed on maps of the Barents Sea. For the whales, D_{ij} represents the number of whales observed within grid cell i in year j in models assuming that the error term e_{ij} followed a Poisson distribution. For the prey species, D_{ij} represents $\log_e$-transformed average acoustic densities within grid cell i in year j in models assuming that e_{ij} followed a normal error distribution. In terms of explanatory variables, year$_j$ is a random factor to adjust for annual variation in average species density, $s(\text{depth}_{ij})$ is a smooth (spline) function of bottom depth in meters at the center of each grid cell, and $s(X_{ij}, Y_{ij})$ is a smooth function of the interaction between X and Y coordinates (in the Lambert equal area projection), which corresponds to the average spatial pattern present across all years of the data set. Additional covariates in the whale models included linear effects of effort (distance in meters along the transect covered by whale observers), Beaufort sea state (BSS) (excluding BSS > 5; WMO 2012) and visibility (distance in m), to take into account observation conditions. These analyses were repeated using 10 × 10 km grid cells, but this change of scale did not alter any results, so the 50 km cells are used in the remainder of the paper. The selected models were used to predict the averaged prey and whale distributions across the study years onto a grid of the study area.

Subsequently, whale densities in the 50 km grid cells were modeled as a response to prey densities, to investigate if the whales were significantly aggregating on specific prey species. Observations of euphausiid backscatter developed in this study allowed this important prey taxon to be included in these models for the first time. These GAMMs were of the form:

$$Y_{ij} \sim \text{factor(year}_j) + \text{effort}_{ij} + \text{visibility}_{ij} + \text{BSS}_{ij} \\ + s(\text{depth}_{ij}) + s(\text{euphausiids}_{ij}) + s(\text{polar cod}_{ij}) \quad (4) \\ + s(\text{capelin}_{ij}) + s(\text{blue whiting}_{ij}) + s(X_{ij}, Y_{ij}) + e_{ij}$$

where Y_{ij} represents the number of whales observed in grid cell i and year j, and modeled as linear effects of BSS, visibility, effort, and smooth functions of bottom depth, average prey densities in grid cell i and year j, and the interaction between X and Y coordinates, assuming that the error term e_{ij} followed a Poisson distribution. Year was entered as a random factor to account for variation in annually averaged whale densities. Models in the form of Eq. (4) were initially fit both with and without the $s(X_{ij}, Y_{ij})$ term. We found that inclusion of this term removed both spatial trends in residuals and the over-dispersion

observed in models without the spatial term (dispersion factors > 1.5): $s(X_{ij}, Y_{ij})$ serves as a proxy for other processes unaccounted for in the models that also influence the whale distributions. The shape of the functional relationships between prey and whales were unaffected by the inclusion of the $s(X_{ij}, Y_{ij})$ term. Model results presented in this paper therefore include the $s(X_{ij}, Y_{ij})$ term. These analyses were also repeated using 10 × 10 km grid cells, but again this change of scale did not alter any results.

Finally, to further investigate the relative influence of capelin and euphausiids as prey, we fit a model that included a term for an interaction between the densities of these taxa when the main effects of these taxa were significant. A smooth interaction term $s(\text{euphausiids}_{ij}, \text{capelin}_{ij})$ was used in place of separate terms for main effects of these prey species, and had the following form:

$$Y_{ij} \sim \text{factor(year}_j) + \text{effort}_{ij} + \text{visibility}_{ij} + \text{BSS}_{ij} \\ + s(\text{depth}_{ij}) + s(\text{euphausiids}_{ij}, \text{capelin}_{ij}) \quad (5) \\ + s(\text{polar cod}_{ij}) + s(\text{blue whiting}_{ij}) + s(X_{ij}, Y_{ij}) + e_{ij}$$

where Y_{ij} represents the number of whales observed in grid cell i and year j, and modeled as linear effects of effort, BSS, visibility, and smooth functions of depth, average densities of krill and capelin in grid cell i and year j, and the interaction between X and Y coordinates, assuming that the error term e_{ij} followed a Poisson distribution. Year was entered as a random factor to account for variation in annually averaged whale densities (e.g. due to changing numbers of whales migrating in and out of the area).

The GAMMs described above were run in R (Version 2.15.2, R Development Core Team 2012), using the gamm4 package (Wood & Scheipl 2013). A backward selection procedure, by removing the least non-significant variables (assuming a significance level of 0.05), was applied to identify the best models. Furthermore, the AIC (Akaike information criterion) was used to compare the models resulting from Eqs. (4) & (5).

RESULTS

Frequency response of euphausiids

The frequency response from the targeted Barents Sea macroplankton trawl (Fig. 2, top panel), whose catch was almost entirely composed of *Thysanoessa inermis*, was very close to the empirical frequency response obtained for *Thysanoessa* spp. euphausiids
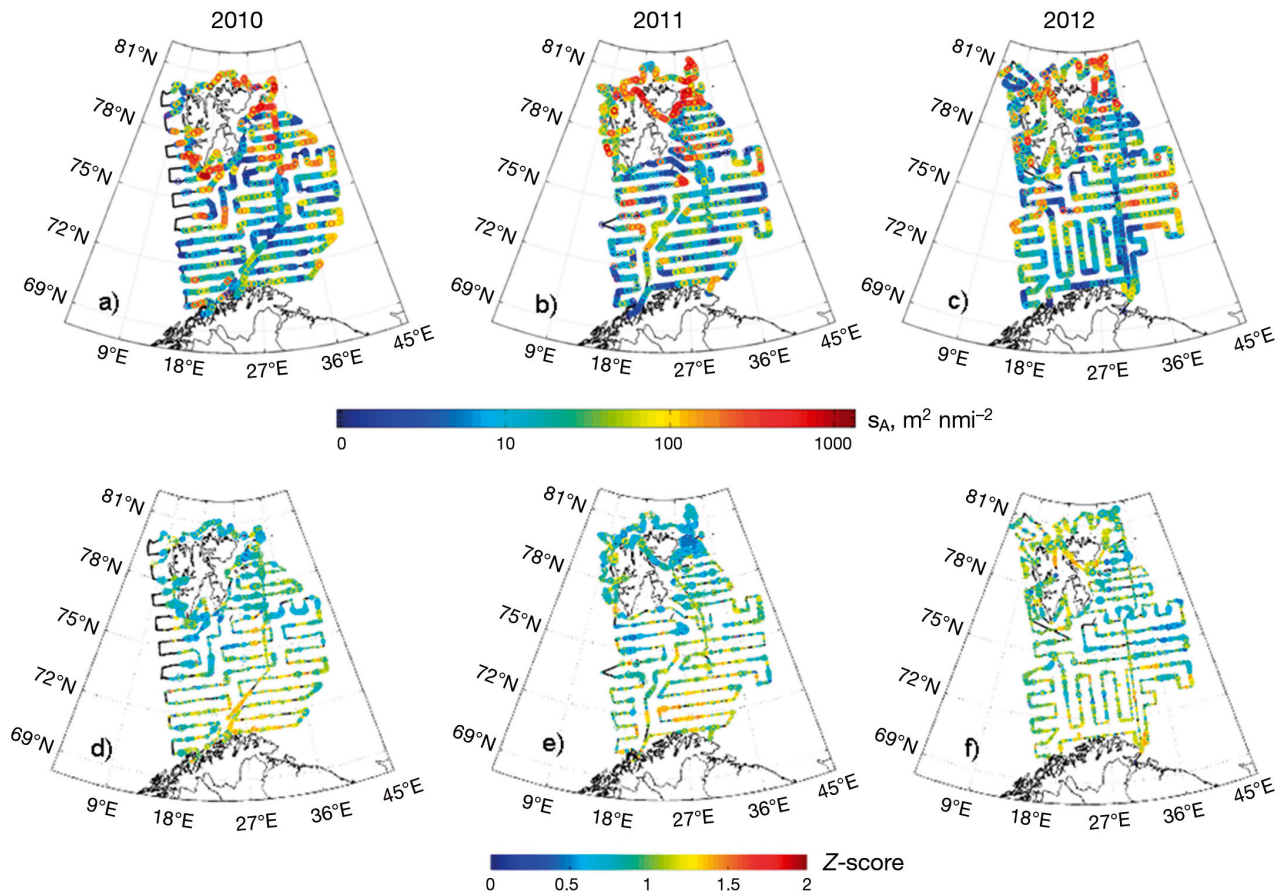
Fig. 3. (a–c) Distribution of $s_{A,euph}$ (m^2 nmi^{-2}) in 2010, 2011, and 2012 (from left to right). Of note are the patchiness of the distribution and the concentration of high values in the northern part of the survey area. (d–f) Weighted average $Z_{120-38,euph}$ in each elementary distance sampling unit. Color indicates $Z_{120-38,euph}$ value, while bubble size is scaled by $s_{A,euph}$. These data indicate a good match with expected $\Delta S_{v,120-38}$ where large amounts of $s_{A,euph}$ were detected

10 to 30 mm in length from the Bering Sea (De Robertis et al. 2010). In the absence of an extensive data set of targeted trawl catches and backscatter from the Barents Sea, this supports our contention that it is reasonable to use $\mu_{120-38,euph}$ and $\sigma_{120-38,euph}$ from De Robertis et al. (2010) for classification of euphausiid backscatter from these surveys. This frequency pair provides a large contrast in expected frequency response for euphausiids (ca. 14 dB). When the backscatter data from the 2011 macroplankton trawl were classified in this way, the resulting echogram of $S_{v,euph}$ appeared to reasonably isolate the scattering from the targeted euphausiid layer (Fig. 2b–f).

Spatial distribution of euphausiid backscatter

Euphausiid backscatter was found throughout the surveyed area, with patches of both very low and very high density (Fig. 3a–c), including high values

clustered in the northern survey area and around Svalbard. Average $Z_{120-38,euph}$ indicated that much of the backscatter was within 1 SD of the expected euphausiid frequency response (Fig. 3d–f), indicating consistency of $S_{v,euph}$ classifications with the ground-truthed empirical data set, both within the surveyed area and among years (average $Z_{120-38,euph}$ among 3 surveys was 0.965, SD = 0.029).

Comparison with MOCNESS catches

A fine-scale, quantitative comparison of $s_{A,euph}$ with vertically integrated euphausiid biomass (g m^{-2}) from MOCNESS samples showed a positive and statistically significant relationship (r^2 = 0.39, p = 0.0134, n = 15 after the removal of 1 outlier). The variability in this regression is substantial (Fig. 4) and may be a function of factors such as spatial differences in average euphausiid size that are not accounted for in the
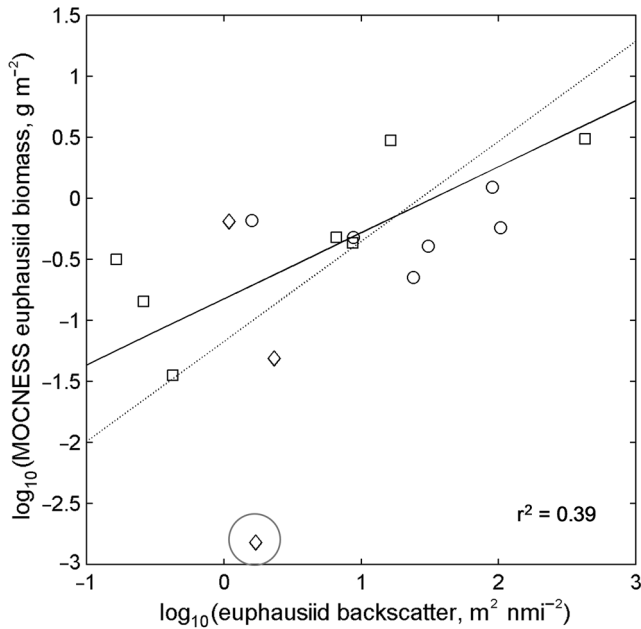
Fig. 4. Vertically integrated biomass of euphausiids *Thysanoessa* spp. from nighttime MOCNESS tows (dry weight, g m^{-2}) is regressed on average vertically integrated daytime euphausiid backscatter ($s_{A,euph}$, m^2 nmi^{-2}) from elementary distance sampling units within 5 nmi of the haul location. Squares, diamonds, and circles indicate data from 2010, 2011, and 2012, respectively. Gray line: regression with all data; black line and r^2 value: regression excluding the circled outlier

fit; thus, caution is required in associating measured backscatter with a particular level of biomass. However, this relationship is consistent with the notion that $s_{A,euph}$ from this analysis provides a relative index of euphausiid biomass.

Euphausiids were the main large crustacean zooplankton (>2 mm) in MOCNESS catches from 2010 to 2012. Based on the same MOCNESS samples used in Fig. 4, dominant euphausiid taxa included *Thysanoessa* spp. (median 79% of euphausiids by number, mainly *T. inermis* and *T. longicaudata*), with an average length of 15.3 mm (SD = 3.9) and *Meganyctiphanes norvegica* (median 4% by number; mean length of 26.4 mm, SD = 8.7). Amphipods *Themisto* spp. in the Barents Sea may be of a roughly similar size (Dalpadado & Skjoldal 1991, 1996, Dalpadado et al. 2001, Dalpadado 2002) and could be acoustically confused with euphausiids, but their abundance and biomass is typically far lower than that of euphausiids throughout most of the sampled area (cf. Dalpadado & Skjoldal 1991, 1996, Dalpadado et al. 2001, Dalpadado 2002, Skern-Mauritzen et al. 2011). This has been particularly true during recent years in the Barents Sea, when warmer than average conditions were

characterized by a reduction in southward intrusion of Arctic waters and in the abundance of one of the major amphipod species in the Barents Sea, *Themisto libellula* (Dalpadado et al. 2012). MOCNESS data from 2010 to 2012 (tows used in Fig. 4) confirm that integrated euphausiid biomass (g m^{-2}) was about 11 times higher than amphipod biomass, on average. Though it is possible that amphipods could have contributed to $s_{A,euph}$ in some areas, we are confident in our interpretation of backscatter classified using the methods described here, i.e. that it principally represents euphausiids and that its use as a measure of the availability of an important type of baleen whale prey is appropriate to our hypothesis.

Euphausiid backscatter as a predictor of baleen whale distribution

The predicted average distributions of baleen whales, euphausiids, capelin, and other potential prey of whales across the study years (made using GAMMs in the form of Eq. 3) are shown in Fig. 5. For all species, the prediction models included depth and $s(X_{ij}, Y_{ij})$ (Tables 1–3), and, for whales, the models also included observer effort, BSS, and visibility data (Tables 1 & 3). At a survey-wide scale, there were some similarities in the average distribution pattern across the study years of $s_{A,euph}$ and the baleen whales (Fig. 5). High densities of all 3 whale species were observed in the northern part of the study area, where dense patches of euphausiids were present (Fig. 5). In particular, high densities of fin and minke whales were observed in areas with high average euphausiid densities, stretching from these northern areas and southeast to Bear Island at the southern end of Svalbard Bank (Figs. 1 & 5). The selected models of baleen whale densities as functions of prey densities indicated significant spatial associations between humpback and fin whales and euphausiids, between all 3 whale species and capelin, and between fin and minke whales and polar cod, whereas no associations with blue whiting were found (Table 3). Models with prey covariates (Table 3) showed significant improvements in the deviance explained (6 to 9% increase) and the AIC score (ΔAIC of 66 to 193; Burnham & Anderson 1998) over models that did not include prey (Table 1). Fin whale densities were positively and linearly associated with euphausiid backscatter densities, whereas humpback whale densities showed a bimodal distribution relative to euphausiid backscatter densities (Fig. 6). We are cautious in interpreting this bimodality, given
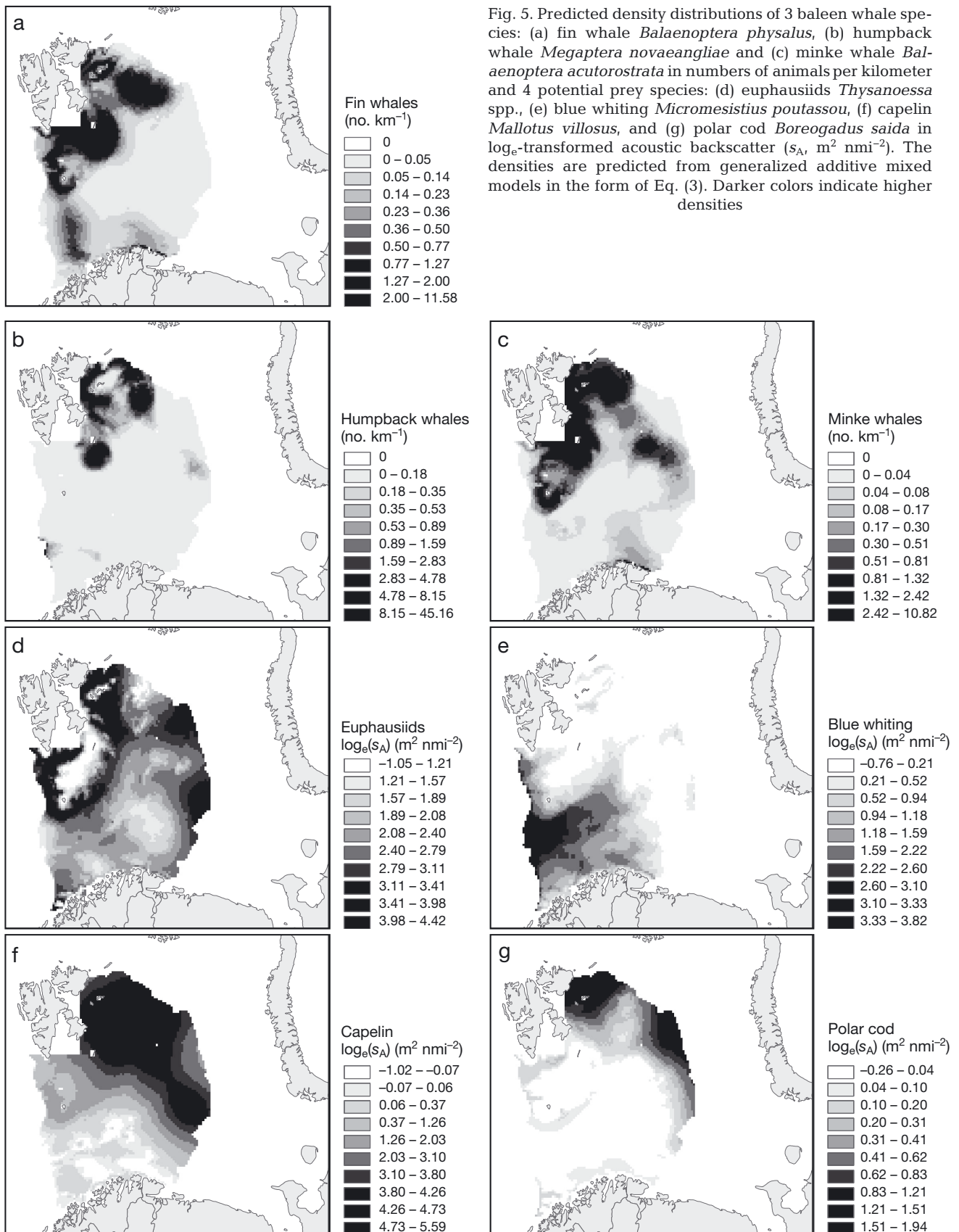
Fig. 5. Predicted density distributions of 3 baleen whale species: (a) fin whale *Balaenoptera physalus*, (b) humpback whale *Megaptera novaeangliae* and (c) minke whale *Balaenoptera acutorostrata* in numbers of animals per kilometer and 4 potential prey species: (d) euphausiids *Thysanoessa* spp., (e) blue whiting *Micromesistius poutassou*, (f) capelin *Mallotus villosus*, and (g) polar cod *Boreogadus saida* in $\log_e$-transformed acoustic backscatter (s_A, m^2 nmi^{-2}). The densities are predicted from generalized additive mixed models in the form of Eq. (3). Darker colors indicate higher densities

the flexibility of the GAMM, the potential for overfitting, and the possibility that this shape could result in part from the geographically limited distribution of humpback whales relative to the distribution of krill (Fig. 5). Thus, we mainly interpret this partial effect to indicate that higher than average densities of humpback whales were found in areas with high euphausiid backscatter, and also that an overall

Table 1. *Balaenoptera acutorostrata*, *Megaptera novaeangliae*, *Balaenoptera physalus*. Summary statistics for whale distribution models (Eq. 3). Covariates included survey effort (distance in meters along the transect covered by whale observers), Beaufort sea state (BSS, 1–12), visibility (distance in meters), depth (m), and spatial location. edf: estimated degrees of freedom; F: Fisher test of significance; p: probability associated with F under the null hypothesis of no significant effect (values in italics are not significant at the 0.05 level, and were not included in the final models); DE: deviance explained by the model; AIC: Akaike information criterion score

	Minke whale			Humpback whale			Fin whale		
	edf	F	p	edf	F	p	edf	F	p
Effort	1	98.97	<0.001	1	20.6	<0.001	1	50.49	<0.001
BSS	*1*	*2.49*	*0.11*	*1*	*0.6*	*0.44*	*1*	*3.31*	*0.07*
Visibility	1	44.42	<0.001	1	19.07	0.001	1	55.23	<0.001
Depth	3.67	40.72	<0.001	1	41.44	0.001	3.65	31.37	<0.001
X,Y	23.63	224.12	<0.001	24.62	384.26	<0.001	22.49	185.45	<0.001
DE		0.55			0.62			0.35	
AIC		780.86			873.68			829.01	

Table 2. *Thysanoessa* spp., *Micromesistius poutassou*, *Mallotus villosus*, *Boreogadus saida*. Summary statistics for prey species distribution models (Eq. 3) of pelagic fish prey (m² nmi⁻²) and euphausiids $s_{A,euph}$ (m² nmi⁻²), and spatial location. Covariates included depth (m) and spatial location. edf: estimated degrees of freedom; F: Fisher test of significance; p: probability associated with F under the null hypothesis of no significant effect; Adj. R²: proportion of variance explained by the model

	Euphausiids			Blue whiting			Capelin			Polar cod		
	edf	F	p	edf	F	p	edf	F	p	edf	F	p
Depth	3.65	31.43	<0.001	3.36	27.3	<0.001	2.38	3.42	0.03	2.22	5.25	0.004
X,Y	22.96	7.78	<0.001	16.79	16.38	<0.001	24.07	43.92	<0.001	23.19	23.48	<0.001
Adj. R2		0.31			0.56			0.71			0.48	

Table 3. *Balaenoptera acutorostrata*, *Megaptera novaeangliae*, *Balaenoptera physalus*. Summary statistics for models of whale densities as a function of prey densities. Covariates included survey effort (distance in meters along the transect covered by whale observers), Beaufort sea state (BSS; 1–12), visibility (distance in meters), depth (m), acoustic backscatter from pelagic fish prey (m² nmi⁻²), euphausiid backscatter $s_{A,euph}$ (m² nmi⁻²), and spatial location. edf: estimated degrees of freedom; F: Fisher test of significance; p: the probability associated with F under the null hypothesis of no significant effect (values in italics are not significant at the 0.05 level, and were not included in the final models); DE: deviance explained by the model; AIC: Akaike information criterion score

| Predictor	Minke whale			Humpback whale			Fin whale		
	edf	F	p	edf	F	p	edf	F	p
Effort	1	96.53	<0.001	1	33.32	<0.001	1	54.06	<0.001
BSS	1	14.77	<0.001	1	4.29	0.04	*1*	*0.05*	*0.83*
Visibility	1	46.95	<0.001	1	13.17	0.002	1	69.49	<0.001
Depth	1	5.74	0.01	1	5.19	0.023	2.4	25.89	<0.001
Euphausiids	*1*	*1.10*	*0.29*	3.91	99.44	<0.001	1	52.69	<0.001
Capelin	3.68	65.63	<0.001	3.92	69.01	<0.001	3.06	12.52	0.006
Polar cod	2.94	30.40	<0.001	*1*	*0.2*	*0.65*	3.33	9.22	0.04
Blue whiting	*1*	*0.38*	*0.29*	–	–	–	*1*	*0.23*	*0.63*
X,Y	20.11	203.49	<0.001	23.36	296.14	<0.001	22.89	178.01	<0.001
DE		0.63			0.71			0.41	
AIC		648.02			680.35			763.17	
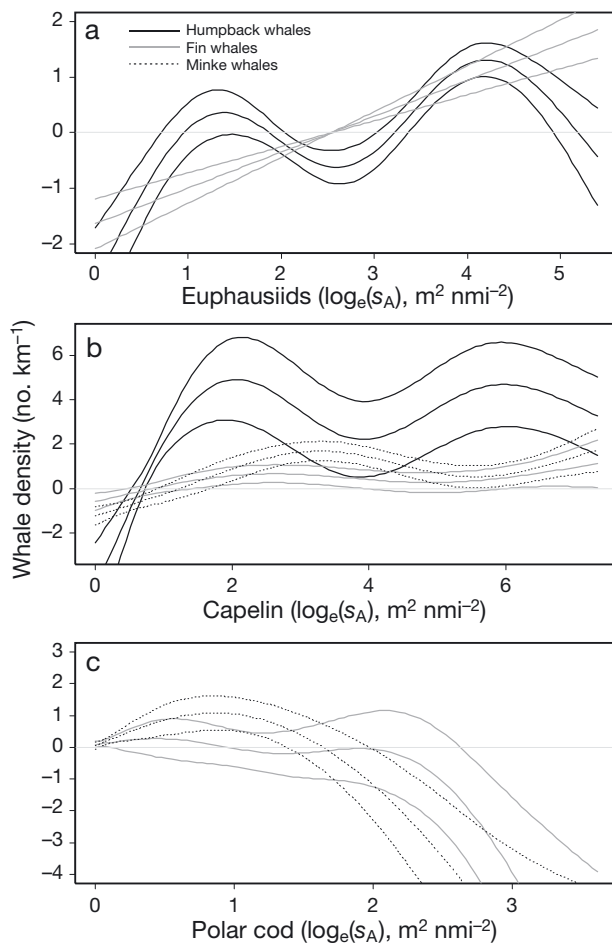
Fig. 6. Partial effect plots of vertically integrated backscatter (s_A) from (a) euphausiids *Thysanoessa* spp., (b) capelin *Mallotus villosus*, and (c) polar cod *Boreogadus saida* on densities of humpback whales *Megaptera novaeangliae*, minke whales *Balaenoptera acutorostrata*, and fin whales *Balaenoptera physalus*. Each plot indicates the mean and 95% confidence interval of the effect of each covariate on predicted density when the effects of other covariates in the model have been held constant (note the $\log_e$ scale). The effects of euphausiids on minke whales and polar cod on humpback whales were not significant in the models and are not shown. The horizontal light grey line indicates mean whale density

increase in humpback whale densities coincided with increasing euphausiid backscatter (Fig. 6). The inclusion of euphausiid backscatter, in particular, improved both deviance explained (4% increase) and the AIC score (ΔAIC of 50 to 89) of models for fin and humpback whales. No association was found between minke whales and euphausiids (Table 3). All 3 whale species were positively associated with capelin, although the functional form differed among the whale species (Fig. 6). While minke and fin whale densities generally increased with increasing capelin densities, the densities of humpbacks increased

abruptly at lower capelin densities and remained significantly above average across a large range of capelin densities (Fig. 6). The densities of fin and minke whales were generally negatively associated with polar cod, whereas no association was found between humpback whales and polar cod.

Since fin whale and humpback whale models indicated significant associations with both euphausiids and capelin, densities for these whales were also modeled using a euphausiid–capelin interaction term in lieu of the corresponding main effects (Eq. 5); the models with the interaction term had slightly, but significantly (ΔAIC of 3 to 6) lower AIC scores than the main effects models (Eq. 4; Fig. 7), though the deviance explained did not change. In many respects, the results from these models differed little from the main effects models; for both species, higher whale densities were predicted at higher densities of euphausiids and capelin (Fig. 7). This suggests that the positive effects of euphausiids and capelin were in large part separate and additive, and the amount of additional explanatory power offered by the introduction of a higher order model term was small. However, the euphausiid–capelin interaction model results (Fig. 7, compare left column with right column) did show some evidence of high whale densities in areas where capelin were absent and euphausiids were present in high densities, but not in areas where euphausiids were absent, even if capelin were present in high densities. This could indicate that the effect of euphausiids on whale density was greater when capelin were scarce.

Finally, since capelin are also a predator of euphausiids, it might be expected that capelin densities and euphausiid densities might be associated in this data set. We tested this idea by adding euphausiid density as a covariate to the capelin distribution model (e.g. added s[euphausiids$_{ij}$] in a model of capelin density of the form of Eq. 3), and found that it was not a significant model term (p > 0.05). The lack of a strong association between euphausiid and capelin densities in this data set is consistent with our interpretation of the euphausiid and capelin effects as separate and additive covariates in the whale distribution models.

DISCUSSION

Interpretation of acoustic backscatter from euphausiids

The distribution of euphausiid backscatter was patchy, but there were consistent areas of dense concentrations in the northern and central parts of the
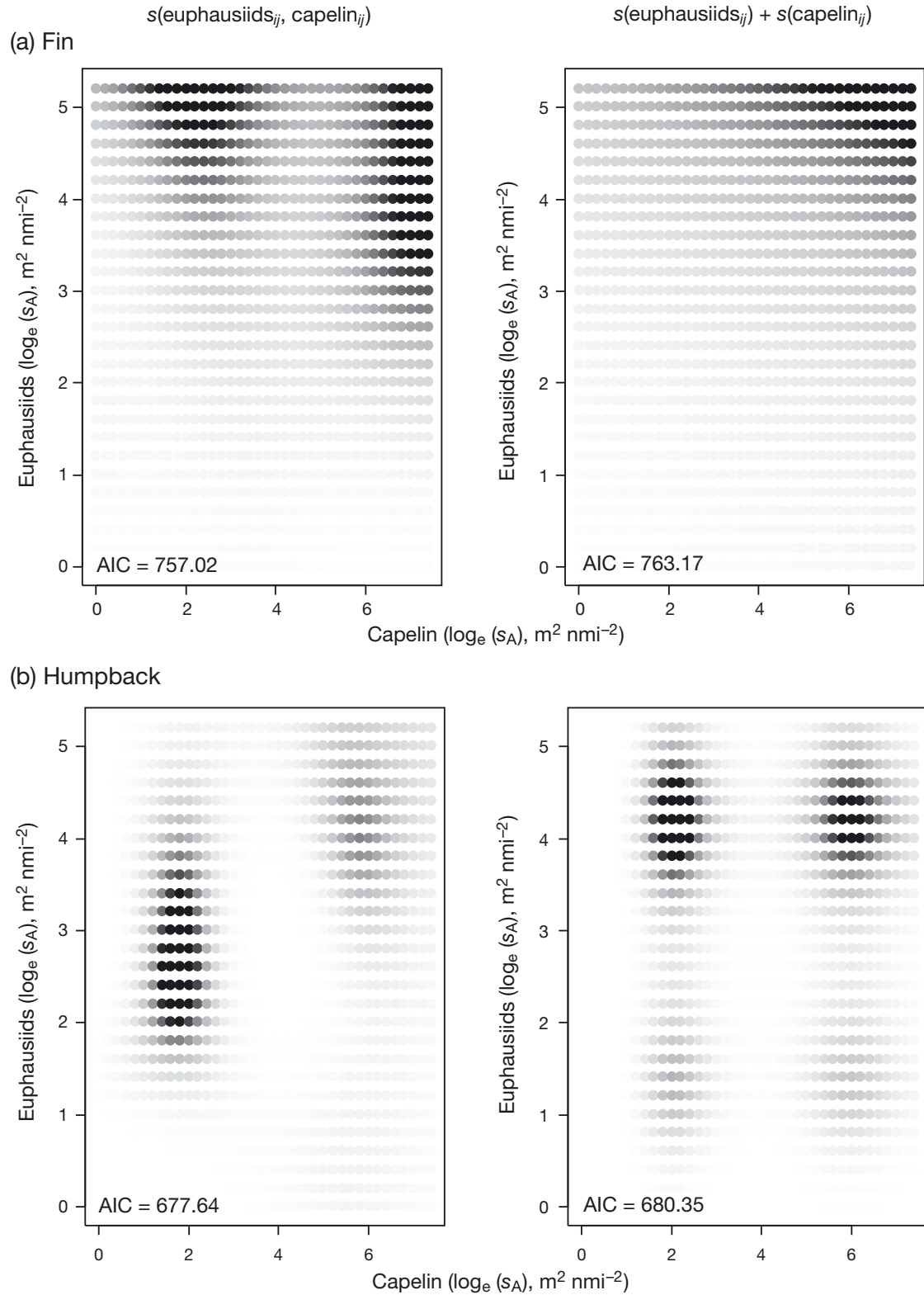
Fig. 7. Predictions of whale density for (a) fin whales *Balaenoptera physalus* and (b) humpback whales *Megaptera novaean-gliae* as a function of the density of euphausiids *Thysanoessa* spp. and capelin *Mallotus villosus*, using models with an inter-action term in lieu of main effects for euphausiids and capelin (left panels; Eq. 5), and models with main effects of euphausiids and capelin only (right panels; Eq. 4). Darker color indicates relatively higher predicted whale densities at a given level of euphausiid and capelin density in each model. AIC: Akaike information criterion score. The effect of euphausiids was not sig-nificant in models of minke whales *Balaenoptera acutorostrata*, so models with interaction between euphausiids and capelin were not used

Barents Sea. These patterns are broadly consistent with the distribution of Barents Sea euphausiids in the literature (Zhukova et al. 2009, Orlova et al. 2011, Skern-Mauritzen et al. 2011, Dalpadado & Mowbray 2013). Spatial patterns in euphausiid backscatter observed in 2010, 2011, and 2012 were correlated with vertically integrated euphausiid biomass collected by MOCNESS plankton nets. These results suggest that euphausiid backscatter can be used as a proxy for euphausiid biomass in the Barents Sea, as is being done in other systems (e.g. Reiss et al. 2008, Ressler et al. 2012, McQuinn et al. 2013). An acoustic approach to surveying euphausiid biomass and distribution has a distinct advantage over other methods: acoustic data provide a substantial increase in spatial and vertical sampling resolution over the spacing among net sample collections of euphausiids in the Barents Sea ecosystem survey (Eriksen & Dalpadado 2011, Olsen et al. 2011, Skern-Mauritzen et al. 2011), complementing the taxonomic resolution of net sampling efforts at a modest increase in cost. A significant amount of time is devoted to quality control and analysis of acoustic backscatter and net sample data for pelagic fishes (Olsen et al. 2011); the similar (but smaller) additional effort required to improve collection of euphausiid acoustic survey data would include devoting survey time to the collection of targeted net samples of acoustic backscatter from euphausiids, additional quality control of all acoustic frequencies used, and post-processing analysis time. A large-scale, high-resolution survey of euphausiids in the Barents Sea could improve the functional understanding of the distribution and abundance of both euphausiids and their predators, including large whales (as we have shown here), seabirds, and commercially important fishes (Dolgov et al. 2011).

Since acoustical properties of euphausiids (or any organism) may vary with size, species, and environmental conditions (e.g. Kristensen & Dalen 1986, McQuinn et al. 2013, Smith et al. 2013), using the backscatter frequency response of euphausiids from the Bering Sea to classify the Barents Sea acoustic data could have introduced error into our index of euphausiid biomass. However, we suspect this error was small in our study, because in both of these seasonally ice-covered, high-latitude ecosystems the dominant euphausiid species and size spectra are similar, and the limited frequency response information we had for Barents Sea euphausiids was consistent with the Bering Sea data we used for classification. The larger euphausiid species *Meganyctiphanes norvegica* is not present in the Bering Sea, but it was typically a very small fraction by number of

the euphausiids in the data set analyzed here. Future work in the Barents Sea would benefit from additional ground-truthing of euphausiid backscatter layers using appropriate nets and/or optical samplers. Length and species composition data obtained from these sources would reduce uncertainty in the interpretation of backscatter patterns by providing additional verification of and possibly improvements to the acoustic classification.

Prediction of baleen whale distribution

The potential utility of large-scale, high-resolution, and high-coverage data on euphausiid distribution was demonstrated by significant improvement in the predictive power of GAMM models of baleen whales when these data were included. All 3 whale species appeared to have higher densities in the northern part of the survey area and were distributed in a similar manner to both euphausiids and capelin (Fig. 5), consistent with what was reported by Skern-Mauritzen et al. (2011). Here, we were able to take advantage of the better spatial coverage of the euphausiid acoustic backscatter data from this study to examine these relationships with pelagic prey at the meso-scale (10 and 50 km grids) as well, which was not previously possible using only net sample euphausiid data. After controlling for depth, location, observation conditions, and the densities of several potential prey taxa, we found that fin whale densities were positively and linearly associated with euphausiid backscatter, and higher than average densities of humpbacks were found in areas with high euphausiid backscatter (Fig. 6). This suggests that both of these whale species aggregate in areas where euphausiids are abundant. No association was found between minke whales and euphausiids. Of the 3 whale species studied, minke whales may be the most piscivorous (Haug et al. 1995), and the lack of association with euphausiids during our study could be explained by the stronger association between minke whales and capelin. Alternatively, Benoit-Bird et al. (2013) have suggested that sometimes other characteristics of prey distribution (e.g. patch characteristics, maximum density) are more important than average prey density in predator–prey relationships; it is possible that this is true for minke whales and euphausiid density as measured here. The density of capelin had a positive effect on all 3 whale species, while polar cod and blue whiting had negative or non-significant effects on whale densities. This is consistent with the hypothesis that capelin are key

prey for all 3 whale species during late summer in the northern Barents Sea.

Baleen whale diets likely exhibit interannual, seasonal, and spatial variability (Haug et al. 2002), but it is clear that capelin and euphausiids are the main prey for baleen whales during late summer in the northern Barents Sea, and are more important than pelagic gadoids (Lindstrøm et al. 1997, Harbitz & Lindstrøm 2001, Lindstrøm & Haug 2001, Skern-Mauritzen et al. 2011). The relative importance of capelin and euphausiids and the influence of prey availability on distribution are difficult to determine (Harbitz & Lindstrøm 2001, Lindstrøm & Haug 2001, Haug et al. 2002). It has been suggested that minke whales might switch from capelin to euphausiids when capelin become less readily available (Skaug et al. 1997, Haug et al. 2002). Smout & Lindstrøm (2007) advocated development of models of foraging whales as a function of their prey distributions, to improve our understanding of functional foraging responses. Skern-Mauritzen et al. (2011) modeled baleen whale distribution during late summer and found ecosystem-scale associations between baleen whales, capelin, and euphausiids, but were not able to test the relative importance of capelin and euphausiids on whale distribution at the mesoscale. The positive association between minke whales and capelin in these models is consistent with the hypothesis that capelin are preferred prey, with euphausiids taken on an opportunistic basis without a strong effect on minke distribution during this time of year. For fin and humpback whales, we propose that our main effect models are the most parsimonious explanation of whale–prey associations in this data set, indicating that these animals prefer to forage where both prey are abundant and available. However, there was some evidence that euphausiid backscatter had a stronger effect upon whale density when capelin were unavailable or at low densities. If euphausiids are somewhat more widely distributed, less patchy, and less able to avoid predators than capelin (a schooling forage fish), perhaps they are more easily obtainable as prey for these whales.

Diets, prey preferences, and foraging behavior of baleen whales are a continuing subject of investigation in other ecosystems as well. Large crustacean zooplankton (e.g. euphausiids) and schooling forage fish (e.g. capelin) have long been considered key prey taxa (Thompson 1940, Jonsgård 1966, Nemoto 1970). In the Gulf of Alaska, humpback whales prey on euphausiids, copepods, capelin, and herring, and may be more likely to eat fish when available (Witteveen et al. 2015, A. M. McCarthy, Alaska Fisheries Science Center, NOAA, pers. comm.); Witteveen et al. (2015) suggested that, although both fin and humpback whales were capable of taking the same prey, differences in their foraging behavior in this system suggested prey partitioning. In the Bering Sea, Sigler et al. (2012) reported that humpback whales were associated with persistent concentrations of euphausiids. A. E. Zerbini et al. (Alaska Fisheries Science Center, NOAA, unpubl. data) found that fin, humpback, and minke whales in the Bering Sea were significantly associated with euphausiid densities, and that the association of minke whales and euphausiids was the weakest of the 3 whale species, similar to observations from our study. Although a preference for fish over zooplankton (when available) is often suspected for baleen whales, inferred foraging preferences for zooplankton and fish vary spatially and seasonally for the same species, consistent with the notion of these whales as flexible, opportunistic predators.

Conclusions

Analysis of multifrequency acoustic backscatter data from the Barents Sea during the period from 2010 to 2012 suggests that acoustic surveys of euphausiid distribution and biomass are feasible. Acoustic backscatter classified as euphausiids was significantly correlated with euphausiid biomass in MOCNESS net catches; combining acoustic and net sampling methods could produce a large-scale index of abundance, biomass, and distribution with high taxonomic and spatial resolution. These data proved useful in fitting multiple regression models of the distribution of fin, humpback, and minke whales, which are all euphausiid predators. Euphausiids and capelin were both significant predictors of baleen whale density. All 3 whale species appear to be opportunistic predators, with capelin a more important predictor of minke whale distribution, and euphausiids and capelin both significant predictors of fin and humpback whale distributions.

cations Group, and 3 anonymous reviewers. The findings and conclusions in the paper are those of the authors and do not necessarily represent the views of the National Marine Fisheries Service.

LITERATURE CITED

Benoit-Bird KJ, Battaile BC, Heppell SA, Hoover B and others (2013) Prey patch patterns predict habitat use by top marine predators with diverse foraging strategies. PLoS ONE 8:e53348

Brierley AS, Watkins JL, Murray AWA (1997) Interannual variability in krill abundance at South Georgia. Mar Ecol Prog Ser 150:87–98

Burnham KP, Anderson DR (1998) Model selection and inference. Springer, New York, NY

Calise L (2009) Multifrequency acoustic target strength of northern krill. PhD thesis, University of Bergen, Bergen

Calise L, Knutsen T (2012) Multifrequency target strength of northern krill (*Meganyctiphanes norvegica*) swimming horizontally. ICES J Mar Sci 69:119–130

Christensen I, Haug T, Øien N (1992) Seasonal distribution, exploitation and present abundance of stocks of large baleen whales (Mysticeti) and sperm whales (*Physeter macrocephalus*) in Norwegian and adjacent waters. ICES J Mar Sci 49:341–355

Clutter RI, Anraku M (1968) Avoidance of samplers. In: Tranter DJ (ed) Zooplankton sampling. Part I: Reviews on zooplankton sampling methods. UNESCO Monograph on Oceanographic Methodology, Vol 2, UNESCO Press, Paris, p 57–76

Coyle KO, Pinchuk AI (2002) The abundance and distribution of euphausiids and zero-age pollock on the inner shelf of the southeast Bering Sea near the Inner Front in 1997−1999. Deep-Sea Res II 49:6009–6030

Dalpadado P (2002) Inter-specific variations in distribution, abundance and possible life cycle patterns of *Themisto* spp. (Amphipoda) in the Barents Sea. Polar Biol 25: 656–666

Dalpadado P, Mowbray F (2013) Comparative analysis of feeding ecology of capelin from two shelf ecosystems, off Newfoundland and in the Barents Sea. Prog Oceanogr 114:97–105

Dalpadado P, Skjoldal HR (1991) Distribution and life history of krill from the Barents Sea. In: Sakshaug E, Hopkins CCE, Øritsland NA (eds) Proceedings of the Pro Mare Symposium on polar marine ecology. Polar Res 10: 443–460

Dalpadado P, Skjoldal HR (1996) Abundance, maturity and growth of the krill species *Thysanoessa inermis* and *T. longicaudata* in the Barents Sea. Mar Ecol Prog Ser 144: 175–183

Dalpadado P, Borkner N, Bogstad B, Mehl S (2001) Distribution of *Themisto* (Amphipoda) spp. in the Barents Sea and predator–prey interactions. ICES J Mar Sci 58: 876–895

Dalpadado P, Ingvaldsen RB, Stige LC, Bogstad B, Knutsen T, Ottersen G, Ellertsen B (2012) Climate effects on Barents Sea ecosystem dynamics. ICES J Mar Sci 69: 1303–1316

De Robertis A, Higginbottom I (2007) A post-processing technique to estimate the signal-to-noise ratio and remove echosounder background noise. ICES J Mar Sci 64: 1282–1291

De Robertis A, McKelvey DR, Ressler PH (2010) Development and application of empirical multifrequency methods for backscatter classification in the North Pacific. Can J Fish Aquat Sci 67:1459–1474

Dolgov AV, Bogstad B, Johannesen E, Skern-Mauritzen M (2011) Trophic relationships. In: Jakobsen T (ed) The Barents Sea ecosystem: Russian–Norwegian cooperation in science and management. Tapir Academic Press, Trondheim, p 431–494

Drobysheva SS (1994) Euphausiids of the Barents Sea and their role for productivity. PINRO, Murmansk (in Russian)

Eriksen E, Dalpadado P (2011) Long-term changes in krill biomass and distribution in the Barents Sea: Are the changes mainly related to capelin stock size and temperature conditions? Polar Biol 34:1399–1409

Ferreira AS de A, Stenevik EK, Vollset KW, Korneliussen R, Folkvord A (2012) Vertical migration of Norwegian spring-spawning herring larvae in relation to predator and prey distribution. Mar Biol Res 8:605–614

Foote KG, Knudsen HP, Vestnes G, MacLennan DN, Simmonds EJ (1987) Calibration of acoustic instruments for fish density estimation: a practical guide. ICES Cooperative Research Report, International Council for the Exploration of the Sea, Copenhagen

Greenlaw CF (1979) Acoustical estimation of zooplankton populations. Limnol Oceanogr 24:226–242

Harbitz A, Lindstrøm U (2001) Stochastic spatial analysis of marine resources with application to minke whales (*Balaenoptera acutorostrata*) foraging: a synoptic case study from the southern Barents Sea. Sarsia 86:485–501

Haug T, Gjøsæter H, Lindstrøm U, Nilssen KT (1995) Diet and food availability for north-east Atlantic minke whales (*Balaenoptera acutorostrata*), during the summer of 1992. ICES J Mar Sci 52:77–86

Haug T, Lindstrøm U, Nilssen KT (2002) Variations in minke whale (*Balaenoptera acutorostrata*) diet and body condition in response to ecosystem changes in the Barents Sea. Sarsia 87:409–422

Heino M, Porteiro FM, Sutton TT, Falkenhaug T, Godø OR, Piatkowski U (2011) Catchability of pelagic trawls for sampling deep-living nekton in the mid-North Atlantic. ICES J Mar Sci 68:377–389

Hewitt RP, Demer DA (2000) The use of acoustic sampling to estimate the dispersion and abundance of euphausiids, with an emphasis on Antarctic krill, *Euphausia superba.* Fish Res 47:215–229

Hewitt RP, Watkins J, Naganobu M, Sushin V and others (2004) Biomass of Antarctic krill in the Scotia Sea in January/February 2000 and its use in revising an estimate of precautionary yield. Deep-Sea Res II 51:1215–1236

Holliday DV, Pieper RE (1995) Bioacoustical oceanography at high frequencies. ICES J Mar Sci 52:279–296

Horne JK (2000) Acoustic approaches to remote species identification: a review. Fish Oceanogr 9:356–371

Johannesen E, Ingvaldsen RB, Bogstad B, Dalpadado P and others (2012) Changes in Barents Sea ecosystem state, 1970–2009: climate fluctuations, human impact, and trophic interactions. ICES J Mar Sci 69:880–889

Jonsgård Å (1966) The distribution of Balaenopteridae in the North Atlantic Ocean. 1966. In: Norris K (ed) Whales, dolphins, and porpoises. University of California Press, Berkeley, CA, p 114–124

Klevjer TA, Kaartvedt S (2006) *In situ* target strength and behaviour of northern krill (*Meganyctiphanes norvegica*). ICES J Mar Sci 63:1726–1735

Korneliussen RJ (2000) Measurement and removal of echo integration noise. ICES J Mar Sci 57:1204−1217

Korneliussen RJ, Ona E (2003) Synthetic echograms generated from the relative frequency response. ICES J Mar Sci 60:636−640

Kristensen Å, Dalen J (1986) Acoustic estimation of size distribution and abundance of zooplankton. J Acoust Soc Am 80:601−611

Lindstrøm U, Haug T (2001) Feeding strategy and prey selectivity in common minke whales (*Balaenoptera acutorostrata*) foraging in the southern Barents Sea during early summer. J Cetacean Res Manag 3:239−249

Lindstrøm U, Haug T, Nilssen KT (1997) Diet studies based on contents from two separate stomach compartments of northeast Atlantic minke whales *Balaenoptera acutorostrata.* Sarsia 82:63−68

McQuinn IH, Dion M, St. Pierre JF (2013) The acoustic multifrequency classification of two sympatric euphausiid species (*Meganyctiphanes norvegica* and *Thysanoessa raschii*), with empirical and SDWBA model validation. ICES J Mar Sci 70:636−649

Michalsen K, Dalpadado P, Eriksen E, Gjøsæter H and others (2013) Marine living resources of the Barents Sea — Ecosystem understanding and monitoring in a climate change perspective. Mar Biol Res 9:932−947

Nemoto T (1970) Feeding patterns of baleen whales in the ocean. In: Steele JH (ed) Marine food chains. University of California Press, Berkeley, CA, p 241−252

Olsen E, Aanes S, Mehl S, Holst JC, Aglen A, Gjøsæter H (2010) Cod, haddock, saithe, herring, and capelin in the Barents Sea and adjacent waters: a review of the biological value of the area. ICES J Mar Sci 67:87−101

Olsen E, Michalsen K, Ushakov NG, Zabavnikov VB (2011) The ecosystem survey. In: Jakobsen T, Ozhigin VK (eds) The Barents Sea. Ecosystem, resources, management. Half a century of Russian−Norwegian cooperation. Tapir Academic Press, Trondheim, p 604−608

Orlova EL, Usakov NG, Nesterova VN, Boitsov VD (2002) Food supply and feeding of capelin (*Mallotus villosus*) of different size in the central latitudinal zone of the Barents Sea during intermediate and warm years. ICES J Mar Sci 59:968−975

Orlova EL, Dalpadado P, Knutsen T, Nesterova VN, Prokopchuk IP (2011) Zooplankton. In: Jakobsen T, Ozhigin VK (eds) The Barents Sea ecosystem: Russian−Norwegian cooperation in science and management. Tapir Academic Press, Trondheim, p 91−119

R Development Core Team (2012) R: a language and environment for statistical computing. R Foundation for Statistical Computing, Vienna. www.r-project.org

Reiss CS, Cossio AM, Loeb V, Demer DA (2008) Variations in the biomass of Antarctic krill (*Euphausia superba*) around the South Shetland Islands, 1996−2006. ICES J Mar Sci 65:497−508

Ressler PH, De Robertis A, Warren JD, Smith JN, Kotwicki S (2012) Developing an acoustic index of euphausiid abundance to understand trophic interactions in the Bering Sea ecosystem. Deep-Sea Res II 65−70:184−195

Ricker WE (1973) Linear regressions in fishery research. J Fish Res Board Can 30:409−434

Sameoto DN, Cochran N, Herman A (1993) Convergence of acoustic, optical, and net-catch estimates of euphausiid abundance: use of artificial light to reduce net avoidance. Can J Fish Aquat Sci 50:334−346

Sameoto D, Wiebe P, Runge J, Postel L, Dunn J, Miller C, Coombs S (2000) Collecting zooplankton. In: Harris RP, Wiebe PH, Lenz J, Skjoldal HR, Huntley M (eds) ICES zooplankton methodology manual. Elsevier, Amsterdam, p 55−81

Sigler M, Kuletz K, Ressler P, Friday N, Wilson C, Zerbini A (2012) Apex predators and hotspot persistence in the southeast Bering Sea. Deep-Sea Res II 65−70:292−303

Simmonds J, MacLennan D (2005) Fisheries acoustics: theory and practice. Blackwell Science, Oxford

Skaug HJ, Gjøsæter H, Haug T, Lindstrøm U, Nilssen KT (1997) Do minke whales (*Balaenoptera acutorostrata*) exhibit particular prey preferences? J Northwest Atl Fish Sci 22:91−104

Skern-Mauritzen M, Johannesen E, Bjørge A, Øien N (2011) Baleen whale distributions and prey associations in the Barents Sea. Mar Ecol Prog Ser 426:289−301

Skjoldal HR, Dalpadado P, Dommasnes A (2004) Food webs and trophic interactions. In: Skjoldal HR (ed) The Norwegian Sea ecosystem. Tapir Academic Press, Trondheim, p 447−506

Smith JN, Ressler PH, Warren JD (2013) A distorted wave Born approximation target strength model for Bering Sea euphausiids. ICES J Mar Sci 70:204−214

Smith SL (1991) Growth, development and distribution of the euphausiids *Thysanoessa raschii* (M. Sars) and *Thysanoessa inermis* (Krøyer) in the southeastern Bering Sea. Polar Res 10:461−478

Smout S, Lindstrøm U (2007) Multispecies functional response of the minke whale *Balaenoptera acutorostrata* based on small-scale foraging studies. Mar Ecol Prog Ser 341:277−291

Thompson RJ (1940) Analysis of stomach contents of whales taken during the years 1937 and 1938 from the North Pacific. MS thesis, University of Washington, Seattle, WA

Wiebe PH, Burt KH, Boyd SH, Morton AW (1975) A multiple opening/closing net and environmental sensing system for sampling zooplankton. J Mar Res 34:313−326

Wiebe PH, Lawson GL, Lavery AC, Copley NJ, Horgan E, Bradley A (2013) Improved agreement of net and acoustical methods for surveying euphausiids by mitigating avoidance using a net-based LED strobe light system. ICES J Mar Sci 70:650−664

Witteveen BH, De Robertis A, Guo L, Wynne KM (2015) Using dive behavior and active acoustics to assess prey use and partitioning by fin and humpback whales near Kodiak Island, Alaska. Mar Mamm Sci 31:255−278

Wood S, Scheipl F (2013) Generalized additive mixed models using mgcv and lme4 (Package gamm4). Available at: http://cran.r-project.org/web/packages/gamm4/

WMO (World Meteorological Organization) (2012) Beaufort Scale of wind force. Appendix I.5, Manual on Marine Meteorological Services, Vol I (Annex VI to WMO Technical Regulations), Global Aspects, No. 558. WMO, Geneva. Available at: http://library.wmo.int/pmb_ged/wmo_558_en-v1.pdf

Zhukova NG, Nesterova VN, Prokopchuk IP, Rudneva GB (2009) Winter distribution of euphausiids (Euphausiacea) in the Barents Sea (2000−2005). Deep-Sea Res II 56:1959−1967